Jurnal Lahan Suboptimal : Journal of Suboptimal Lands
ISSN: 2252-6188 (Print), ISSN: 2302-3015 (Online, https://jlsuboptimal.unsri.ac.id/index.php/jlso)
Vol. 15, No.1: 7–20 April 2026
DOI: 10.36706/JLSO.15.1.2026.783

GIS–MCDA–based land suitability analysis for agrivoltaic development on degraded peatlands in South Sumatra

Muaffan Alfaiz Wisaksono[*)]
Master's Programme in Precision Agriculture, Faculty of Agribusiness and Commerce, Lincoln University, Ellesmere Junction Road, Lincoln 7647, Lincoln, New Zealand
[*)]Email address: muaffan.wisaksono@lincolnuni.ac.nz

(Received: 22 October 2025, Revision accepted: 10 March 2026)

Citation: Wisaksono, M. A. (2026). GIS–MCDA–based land suitability analysis for agrivoltaic development on degraded peatlands in South Sumatra. *Jurnal Lahan Suboptimal : Journal of Suboptimal Lands. 15*(1): 7–20. https://doi.org/10.36706/JLSO.15.1.2026.783

ABSTRACT

Degraded peatlands in South Sumatra experience drainage driven subsidence, recurrent fires, and seasonal flooding, yet they also have reliable long term solar resources, making them strong candidates for agrivoltaics that avoids conversion of intact peat. This study aimed to map and quantify agrivoltaic land suitability on degraded peatlands using an integrated GIS and multi-criteria decision analysis workflow. Eight criteria were prepared on a 30 m UTM Zone 48S grid and normalized to a 0 to 1 benefit scale: FRP weighted fire kernel density, peat depth class as a geotechnical proxy, flood hazard index, slope, distance to roads, aspect, topographic position index, and long term global horizontal irradiance. Weights were derived with the Analytic Hierarchy Process (CR= 0.00244) and combined using Weighted Linear Combination with protected areas applied as hard constraints. Across the eligible degraded peat domain (124,007.76 ha), 53.76% (66,665.25 ha) was very suitable and 24.89% (30,867.84 ha) was moderately suitable, while 19.68% (24,408.99 ha) and 1.67% (2,065.68 ha) were unsuitable and very unsuitable. Overall, 78.65% (97,533.09 ha) of eligible land was suitable or very suitable, indicating a substantial opportunity for policy-focused agrivoltaic screening on degraded peatlands while maintaining environmental safeguards.

Keywords: agrivoltaic, analytic hierarchy process, fire radiative power, geographic information system, global horizontal irradiance

INTRODUCTION

Limiting global warming requires accelerating the transition toward low-carbon energy systems. The Intergovernmental Panel on Climate Change (IPCC) (2022; 2023) emphasizes that mitigation demands large-scale renewable deployment without compromising food systems and ecological integrity. Utility-scale solar photovoltaic (PV) plants are among the most cost-effective options for decarbonizing electricity generation (International Energy Agency, 2023), but ground-mounted PV can compete with agriculture, conservation, and residential development (Hernandez et al., 2015).

Agrivoltaics addresses this tension by co-locating PV electricity generation with agricultural production. Beyond providing clean energy, PV structures can modify microclimatic conditions through partial shading, reducing drought stress and heat on crops and helping sustain productivity (Amaducci et al., 2018; Barron-Gafford et al., 2019). Studies show that adequate module elevation and wider row spacing can improve growing conditions without major losses in energy output (Dinesh & Pearce, 2016; Weselek et al., 2021). This reframes the "food or energy" narrative into a co-benefit paradigm for food, energy, and water security, which is especially relevant for vulnerable ecosystems such as peatlands and other suboptimal lands.

Peatlands store exceptionally high carbon reserves per unit area and play a crucial role in regulating the climate and hydrological cycles (Joosten et al., 2016). In South Sumatra alone, there are approximately 1.2 to 1.5 million hectares of peatlands which have been documented (Finlayson, 2021), with Ogan Komering Ilir Regency accounting for roughly

half of the province's peatland (Irfan et al., 2025). Simultaneously, a substantial solar potential exists in the region with an average Global Horizontal Irradiance (GHI) of approximately 4.8 kWh/m²/day and local peak values reaching about 5.15 kWh/m²/day (Kurniawan et al., 2024), which is consistent with the Global Solar Atlas characterization for the South Sumatra region (World Bank, ESMAP & Solargis, 2023). Land suitability assessment is commonly implemented using Multi-Criteria Decision Analysis (MCDA) within a Geographic Information System (GIS), enabling multiple criteria to be standardized and combined through weighted overlays (Kocabaldır et al., 2023). A widely used weighting approach is the Analytic Hierarchy Process (AHP) developed by Saaty (1980; 2008), which applies pairwise comparisons and checks judgment consistency using the Consistency Ratio (CR). In PV planning, AHP supports transparent weight assignment and sensitivity testing, but its reliability depends on robust spatial datasets and clearly defined constraints (Kırcalı & Selim, 2021).

Despite rapid growth in agrivoltaics research, a gap remains in GIS-AHP suitability studies that explicitly reflect agrivoltaic priorities on degraded peatlands. Integrated analyses that combine multi-year fire density, flood proxies, topographic position indices, accessibility metrics, protected-area buffers, and explicit solar radiation potential in a single AHP-based overlay are still limited. This study develops a replicable screening pipeline that produces suitability maps with transparent classifications and clearly documented assumptions, spatial resolution, and data lineage. Accordingly, this research aimed to compile and standardize key biophysical risk and resource criteria for degraded peatlands in South Sumatra, derive criterion weights using AHP and integrate them in a GIS-based weighted overlay with explicit protection constraints, and map and quantify agrivoltaic suitability classes to support policy-oriented site screening and planning for future references.

MATERIALS AND METHODS

GIS–AHP–MCDA Framework

The agrivoltaic suitability analysis was conducted within the administrative boundaries of South Sumatra using ArcGIS Pro for all spatial processing tasks (environment settings: UTM Zone 48S; cell size: 30 m), AHP was used for deriving weights and calculating the Consistency Ratio (CR), and a Weighted Linear Combination (WLC) approach used to integrate all criteria layers. The GIS-MCDA framework was chosen for its proven reliability in large-scale PV site suitability previous studies across diverse climatic topographic contexts. However, most existing literature covers case studies focusing on arid or semi-arid regions and non-peatland sites such as Saudi Arabia, Turkey, the Mediterranean Basin, Iran, Mauritius, Morocco, Serbia, and Spain, where criteria selection and weighting schemes are highly dependent on local conditions and stakeholder priorities (e.g., GHI, grid proximity, road access, noise, dust exposure, slope, and land use/land cover) (Al Garni & Awasthi, 2017; Çolak et al., 2020; Giamalaki & Tsoutsos, 2019; Doorga et al., 2019; Yousefi et al., 2018; Doljak & Stanojević, 2017; Zoghi et al., 2017; Merrouni et al., 2018; Noorollahi et al., 2016; Kırcalı & Selim, 2021).

Consistent with these cross-literatures findings, no universal protocol had existed for exact weight determination. While GHI often dominate the criteria for national or provincial scales, other factors could be assigned greater weight when policy objectives, local risk factors, or infrastructure constraints are more critical such as dust storm exposure in Isfahan or grid proximity in Cartagena (Zoghi et al., 2017; Kırcalı & Selim, 2021; Doorga et al., 2019). In the context of this study, the generic framework was substantially modified to reflect the distinct biophysical and socio-environmental conditions of degraded peatlands and factors that might affect crop productivity. The analysis was mask restricted exclusively to degraded peatland, protected areas were treated as hard constraints, and the selected criteria emphasized recurring fire risk (using Fire Radiative Power [FRP]-weighted Kernel Density Estimation [KDE]), flood vulnerability, peat depth (linked to geotechnical stability and subsidence risk), slope, topographic position, and accessibility. GHI was applied in weight second to constraints to retain the solar energy potential (ESMAP, 2019a).

The rationale behind this site-specific criteria selection and weighting was significantly influenced by potential suitability to peatland

ecosystems, which were inherently vulnerable to fire, flooding, and subsidence, leading to FRP-weighted fire risk, flood index, and peat depth received higher weights relative to GHI. Slope, Topographic Position Index (TPI), road proximity, and aspect served as secondary filters to assess land flatness, topographic position (e.g., dome crest vs. slope base), and access proximity for yield logistical purpose, before the solar gradient further enhanced the suitability of already "buildable" pixels. This design follows the MCDA siting logic, which prioritizes feasibility and risk envelopes before resource optimization, while remaining consistent with established GIS–AHP best practices (Al Garni & Awasthi, 2017; Çolak et al., 2020; Doorga et al., 2019; Doljak & Stanojević, 2017; Merrouni et al., 2018).

Criteria normalization (0–1, benefit-oriented), reclassification into suitability levels (1–4), generation of distance surfaces, derivation of DEM-based variables (slope, aspect, TPI), kernel density analysis (for fire risk), application of masks and constraints, and execution of the WLC model were all performed ArcGIS Pro. AHP was implemented for pairwise comparisons, eigenvector weight derivation, and CR calculation, ensuring that the entire analytical pipeline was traceable and replicable (Goepel, 2018). All operations used raster analysis to make an easier approach by using a raster calculator, while the application of data and weighing was properly decided by the emphasis received from previous relevant studies.

Table 1. AHP weighting factors used in this study (degraded peatlands, South Sumatra) and their counterparts in general utility-scale PV siting studies

Evaluation criterion (this study)	Direction*	Data source (30 m unless noted)	AHP weight	Counterpart in general PV siting studies	Typical emphasis in the literature
Fire hazard (FRP-weighted KDE, 10-year record)	↓	NASA FIRMS (VIIRS 375 m) + attribute FRP	0.1965	Climate/vegetation risk (rarely explicit "fire")	Low to very low
Peat depth (geotechnical proxy)	↓	Balai Besar Sumberdaya Lahan Pertanian – Kementan (BBSDLP/MoA)	0.1781	Elevation/soil/stability (generic)	Low
Flood Vulnerability Index (hazard)	↓	BNPB – InaRISK Geoservices	0.1599	Flood vulnerability index (subset of studies)	Low to moderate
Slope (gradient)	↑	DEM: Badan Informasi Geospasial (BIG)	0.1412	Elevation/slope	Low to moderate
Proximity to roads	↑	OpenStreetMap (Geofabrik)	0.1216	Proximity to roads/infrastructure	Low to moderate
Aspect	↑	Same DEM	0.0573	Site orientation/aspects	Low
Topographic Position Index (TPI)	↑ (convexity inverted)	Same DEM	0.0355	Micro-relief/landform (seldom used)	Rare
Global Horizontal Irradiance (GHI)	↑	Global Solar Atlas v2 – World Bank / ESMAP / Solargis	0.1099	Solar resource (irradiance)	Tinggi
Not used (rationale)					
Temperature / humidity / cloudiness / dust	—	— (represented implicitly by long-term GHI)	—	Temperature / humidity / cloudiness / dust	Low to moderate
Proximity to settlements	—	— (represented via protected-area buffers, open water, and peat mask)	—	Proximity to settlements	Low

*Criterion direction: ↑ = benefit (larger values imply greater suitability); ↓ = cost (normalized by benefit-type inversion before overlay). Weights were derived from an 8×8 AHP matrix ($\lambda_{max} \approx 8.0241$; CI ≈ 0.00344; CR ≈ 0.00244), satisfying standard consistency requirements. The "general PV" reference for typical weight emphases were informed by Kırcalı & Selim (2021), Al Garni & Awasthi (2017), Doorga et al. (2019), Doljak & Stanojević (2017), Zoghi et al. (2017), and Noorollahi et al. (2016). The scheme above is modified for degraded peatlands by elevating the priority of fire risk, geotechnical risk (peat depth), and flooding (Hooijer et al., 2012; Mezbahuddin et al., 2023) and by adding TPI as a landform filter.

Table 1 summarizes the spatial datasets and AHP-derived weight assignments while linking them to state-of-the-art research, and Figure 1 presented the methodological workflow diagram employed in this study.

A methodological novelty of this study lies in the incorporation of FRP-weighted fire history as a spatial criterion. The fire index was derived using Kernel Density Estimation (KDE) weighted by Fire Radiative Power (FRP), a well-established proxy for combustion intensity and biomass consumption rates (Giglio et al., 2016). By weighting fire hotspots based on FRP rather than frequency alone, the KDE model maps the spatial persistence of high-intensity fires from multi-year active fire records, enabling more accurate identification of areas with recurrent fire risk (Baykal et al., 2025; Deng et al., 2025). This approach supports a more realistic fire risk weighting framework within agrivoltaic site assessments on peatlands.

In addition to FRP, peat depth was incorporated as a non-generic criterion due to its direct implications for geotechnical stability, foundation design, and subsidence risk at PV installation sites (Vernimmen et al., 2020).

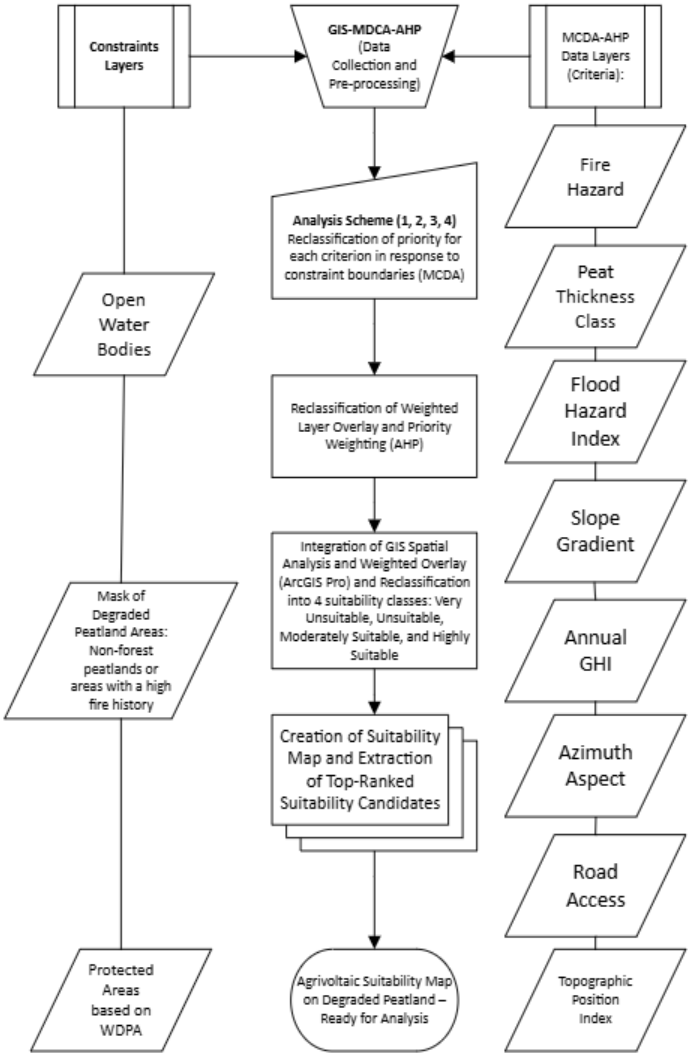

Figure 1. GIS-MCDA-AHP workflow made for agrivoltaic suitability mapping on degraded peatlands in South Sumatra

Hard Constraints (Constraint Layers)

The first step involved defining areas to be excluded from agrivoltaic development based on ecological protection and regulatory restrictions. These constraint layers encompassed conservation and protected areas (World Database on Protected Areas (WDPA), wildlife reserves, and national parks), bodies of water and buffer zones, irrigated rice fields, customary or cultural forests, riparian and canal setbacks from the Land Use Land Cover data, and safety buffers surrounding arterial roads. All spatial datasets were compiled from official ministries, technical agencies, and verified regional data sources to comply with equired analytical precision.

All vector constraint layers were projected into a common topology, converted into 30 m raster grids, and merged through a union operation to generate a single Constraint Mask. This mask was applied prior to suitability classification to ensure that legally restricted areas did not influence the calculation of the Suitability Index (SI). Figure 2 illustrates the spatial distribution of excluded zones—which, in this case study, eliminated a significant proportion of the total land area—along with the exclusion percentage by category (conservation zones, water bodies, paddy fields, customary forests, deep peat deposits, and WDPA-registered protected areas). The inclusion of hard constraints ensures that the proposed agrivoltaic design adheres to environmental and social boundaries from the outset, thereby minimizing location bias caused by the overlay of positive criteria within zones that were legally off-limits and irrelevant with the study.

Evaluation Criteria and Suitability Classification

The first evaluation criterion focused on fire risk, which was developed to capture the potential threats posed by peatland fires to safety, operational continuity, mitigation costs, and emissions. The dataset consisted of all NASA FIRMS (MODIS/VIIRS) satellite-detected hotspots from the past ten years, which were merged, projected into the UTM Zone 48S coordinate system, and processed using a Fire Radiative Power (FRP)-weighted kernel density estimation (KDE) with a five-kilometre search radius. The resulting density layer was scaled to a 0–1 range and inverted so that higher values represented locations with lower fire risk and, therefore, higher suitability.

The second criterion addressed peat depth, serving as a proxy for geotechnical risk such as bearing capacity and foundation requirements. The peatland boundaries were derived from the 2012 National Peatland Map published by the Ministry of Agriculture (BBSDLP), which was the most comprehensive dataset available at the time of analysis. As no spatially uniform, up-to-date numerical peat depth data exist, depth was approximated morphometrically: the distance of each cell from the peatland edge was measured, with greater distances into the dome interior interpreted as relatively thicker peat deposits. These values were then converted into a suitability index, where deeper peat corresponded to lower suitability scores. The third criterion incorporates a flood vulnerability index or groundwater level indicator sourced from the InaRISK–BNPB geospatial service, aligned with the project's spatial resolution and projection parameters. Topography, accessibility, and energy components were derived from five thematic maps, all standardized to a 30-m resolution grid in the UTM 48S projection. First, a slope map was generated from the DEMNAS digital elevation model (0.27″ resolution, EGM2008 datum) and converted to a suitability scale, with gentler slopes receiving higher scores due to reduced earthwork requirements and increased site stability. Second, a slope aspect map derived from the same DEM was classified so that orientations that maximize average daily solar radiation in low-latitude regions were given higher scores. Third, the TPI was calculated to identify micro-topographic features such as depressions, flat surfaces, and ridges; more stable landforms not located on the tops of convex domes were given higher suitability scores. Fourth, a road accessibility map is created by calculating the Euclidean distance from the main road network extracted from OpenStreetMap (2025).

These distances were normalized so that locations closer to roads—associated with lower construction and operational logistics costs—

scored higher. Fifth, a solar potential map was developed by classifying Global Horizontal Irradiance (GHI) values into classes of equal area, with higher values indicating greater energy potential. The eight thematic layers were normalized to a consistent scale and integrated using AHP-based weighted linear combinations to produce the final suitability index. The thematic map obtained from this process was illustrated in Figure 3.

Implementation of AHP and Weighting

The weighting process was carried out through pairwise comparisons of all factors considered in the model, including fire risk, peat depth, flood vulnerability or groundwater level, slope gradient, road accessibility, global solar radiation intensity (GHI), slope aspect, and Topographic Position Index (TPI). Assessments were conducted using a Likert scale of 1–9 to represented the relative importance of each criterion compared to the others. The resulting priority matrix was then normalized by dividing each column element by the total number of elements in that column, then calculating the average of each row to obtain the relative weight of each factor.

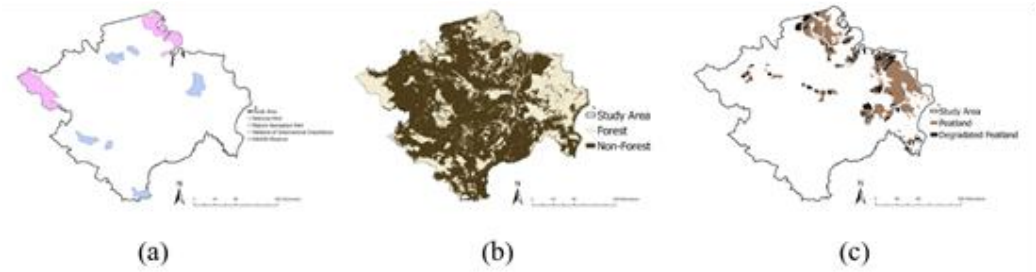

Figure 2. Supporting thematic maps used in site screening: (a) Protected Areas (WDPA), (b) Land Cover (Ministry of Environment and Forestry of the Republic of Indonesia, 2017), and (c) Distribution of Degraded and Non-Degraded Peatlands in South Sumatra.

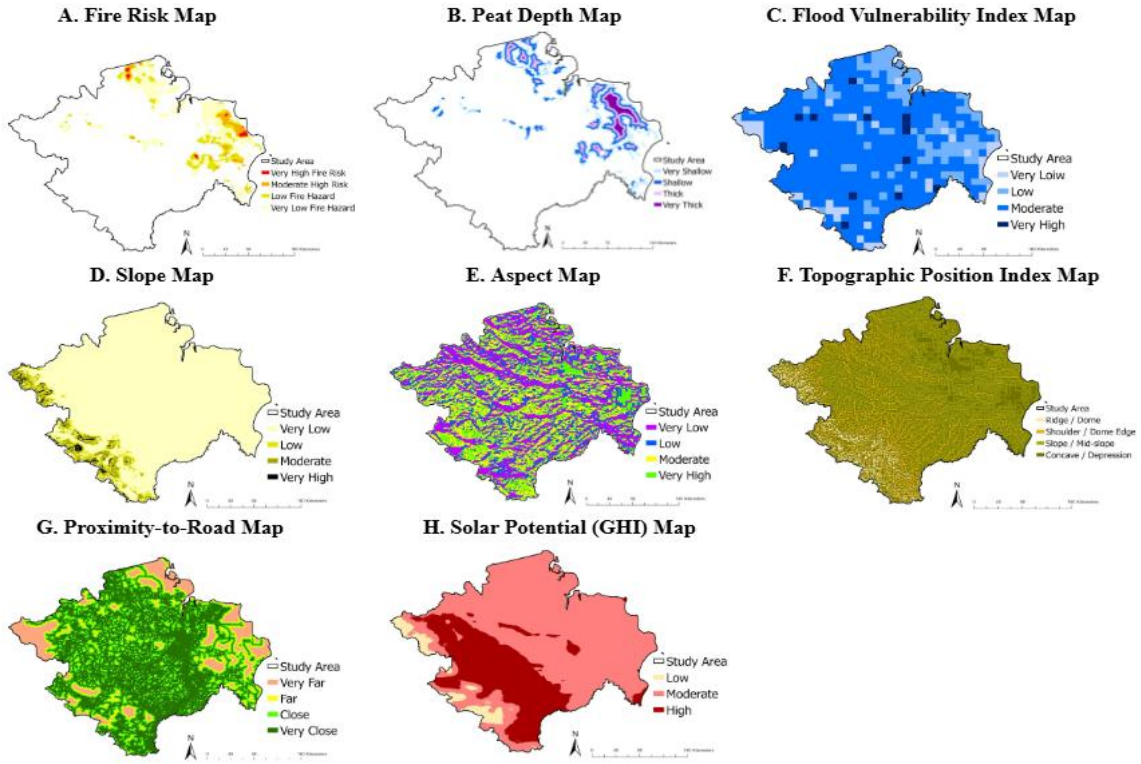

Figure 3. Eight standardized thematic input layers forming the basis of GIS-AHP-MCDA-based agrivoltaic suitability

To ensure internal consistency of the assessment, the Consistency Index (CI) was calculated using the following formula:

$$CI = \frac{\lambda max - n}{n - 1}, \quad (1)$$

where λ_{max} was the maximum eigenvalue of the comparison matrix and n was the number of criteria, and the Consistency Ratio (CR) was then determined as CR = CI/RI, where RI represented Saaty's random index corresponding to the matrix size n. All sets of weights were considered valid if CR $\leq$ 0.05; if this threshold was exceeded, the pairwise comparison process was repeated until consistency was achieved.

Weighted Overlay and Suitability Index Classification

All thematic layers were first standardized to a common scale through reclassification. They were then integrated using a weighted overlay model to generate the Suitability Index (SI) for each pixel, expressed as:

$$SI = \sum_{i=1}^{m} w_i . x_i, \quad (2)$$

where w_i was the AHP-derived weight of factor *i* and x_i was the standardized class score of factor *i*, were categorized into four classes for planning purposes: Low (1–3), Moderate (3–5), Suitable (5–7), and Highly Suitable (7–9). Class thresholds were determined using the natural breaks (Jenks) classification method to ensure statistical robustness, and hard constraints such as protected areas, buffer zones, and safety setbacks were applied post-overlay to ensure that restricted zones were excluded from the pool of potential development sites.

Final Suitability Maps and Post-Constraint Statistics

The primary output of this analysis was a post-constraint suitability map categorized as "Very Suitable," highlighting only the most optimal locations after all protected areas, riparian zones, and safety buffers have been excluded in the area analysis. The map was complemented by descriptive statistics that include the total area (km²) and its percentage of the total study area, as well as the number and size of suitability clusters (patches) that illustrate the scale and spatial distribution of potential projects. As an additional metric to support decision-making, an estimated installed capacity is also calculated specifically for the "Very Suitable" area using a surface-area-based approach. In this approach, capacity (MW) was estimated by multiplying the total effective area (km²) by the conservation agrivoltaic power density (MW/km²), adjusted for system design parameters such as panel row spacing, ground coverage ratio (GCR), and the need for cultivation alleys. These estimates provide a practical reference for policymakers and investors to assess the potential scale and feasibility of implementing agrivoltaic systems on degraded peatlands.

RESULTS

Suitability Class Distribution within the Analysis Domain

The suitability raster produced four classes (1–4). Areas were computed consistently using a 30 m pixel size (0.09 ha per pixel). The total classified surface comprises 1,377,864 pixels or 124,007.76 ha, while the aggregate extents of intact peatland and degraded peatland captured in the analysis measure 861,331.50 ha and 230,810.25 ha, respectively. The number of the peatland covered in the study area should be highlighted as it used a 2012 data and under the context of peatland as peat soils, not peat ecology which could include larger areas. The area and percentage distribution for each suitability class were presented in Table 2, the extents of intact and degraded peatland masks were summarized in Table 3, and the spatial outcome of the suitability analysis was illustrated in Figure 4.

Table 2. Distribution of suitability classes within the analysis domain

Class	Category	Area (ha)	Percentage (%)
1	Very low	2,065.68	1.67
2	Low	24,408.99	19.69
3	Moderately suitable	30,867.84	24.89
4	Highly suitable	66,665.25	53.76
	Total	124,007.76	100.00

A concise numerical summary indicates the dominance of the "Highly Suitable" class at 53.76 percent of the classified surface, followed by "Moderately Suitable" at 24.89 percent, "Low" at 19.69 percent, and "Very Low" at 1.67 percent. Which gives an optimistic view in regard to the agrivoltaic possibilities in the degraded peatland in South Sumatra as there were a high number of highly suitable areas.

The four-class agrivoltaic suitability map within the peatland domain reveals distinct spatial clustering of "Highly Suitable" pixels across several lowland peat blocks, with two major clusters highlighted in insets at a scale of approximately 5–9 km. Other suitability classes—"Low" and "Moderate"—form transitional belts surrounding the bright green core clusters, while "Very Low" suitability areas were comparatively rare and scattered.

Table 3. Area distribution of the peatland mask

Value	Meaning	Area (ha)
1	Intact peatland (non-degraded)	861,331.50
0	Degraded peatland	230,810.25
	Total	1,092,141.75

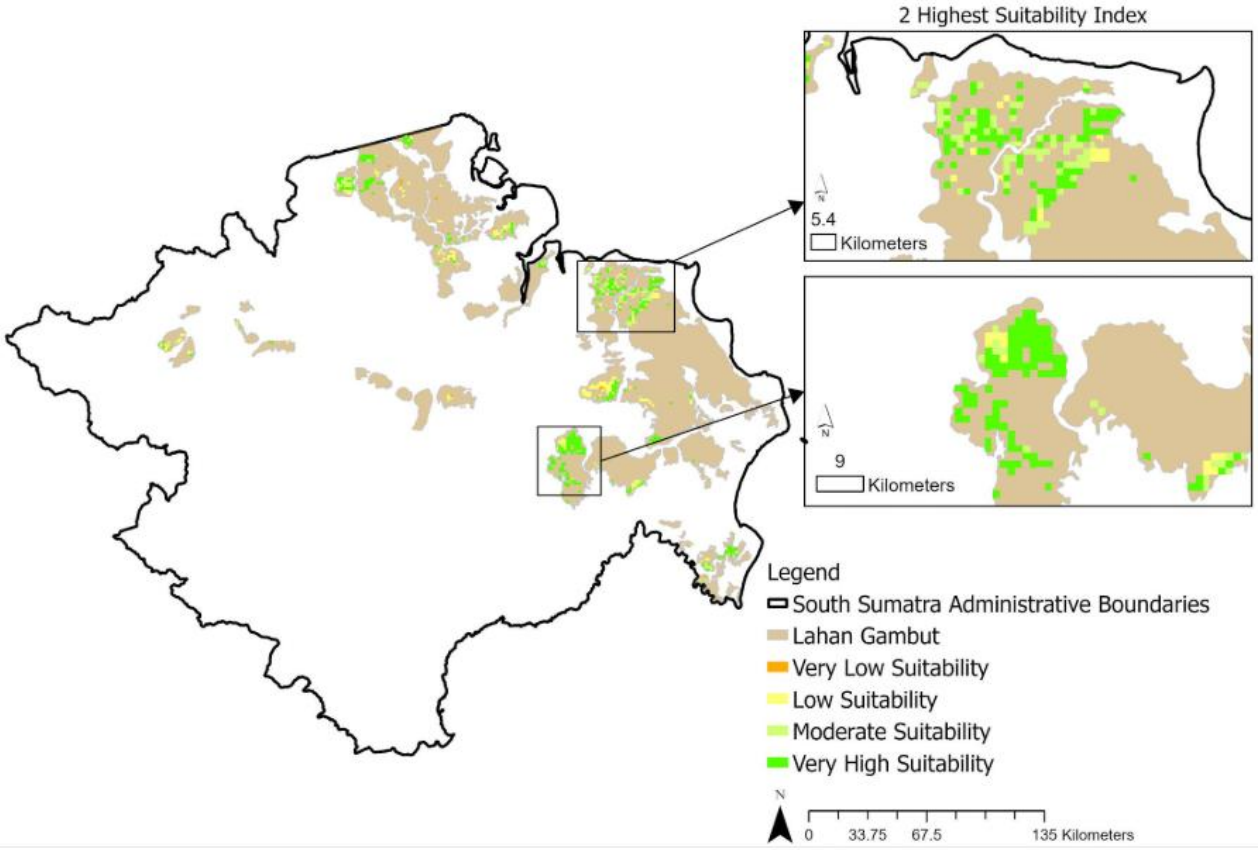

Figure 4. Four-class agrivoltaic suitability map over peatlands in South Sumatra; insets highlight two clusters of th highest suitability.

DISCUSSION

Spatial Patterns and Suitability Structure

A distinct spatial pattern emerges, where over half the area (53.76) falls into the "Highly Suitable" category, surrounded by "Moderately Suitable" areas (24.89%), forming a two-layered spatial structure: a contagious high-suitability core located in low-lying peatland plains, encircled by a transitional moderate-suitability belt. The presence of the fragmented "Low" (19.69%) and "Very Low" (1.67%) suggest localized challenges such as uneven ground, poor access routes, or lingering environmental risks. Spatially, the the centroid of suitability tends to shift towards the east-southeast clusters of the peatland domain, characterized by gentler topography, better road proximity, and minimal multi-year hazard footprints. In these areas, GHI plays a supportive role rather than being the sole driver of suitability, meaning that suitability peaks are formed by areas with most feasible conditions for initial development. This spatial structure is particularly significant as it indicates spatial resilience, reflected in the consistency of high-suitability scores across several kilometers, which would benefit project block planning, construction logistics, and long-term operational management. Key clusters are concentrated in the central-easter parts of South Sumatra, particularly in Central-Eastern Banyuasin, Northern Ogan Komering Ilir (OKI), Northern Ogan Ilir, and Eastern Muara Enim. These zones are characterized by flat topography (<3%), medium peat depth (around 50–150 cm), strong infrastructure links, and steady solar exposure. Surrounding these prime zones, Moderately Suitable areas extend across Southern OKI, Southern Musi Banyuasin, and parts of Eastern Banyuasin, where deeper peat layers and seasonal flooding create natural boundaries. The appearance of highly suitable areas is not simply driven from "GHI monoculture" but rather the outcome of a sequential screening process in which persistent peat fire patterns (derived by multi-year FRP-weighted KDE), flood risk indicators, and peat depth serves as primary filters, while GHI serves as the secondary booster once risk and constructability criteria are met. Global hydrological risk literature highlights that flood events tend to persist and intensify in low-lying regions (Alfieri et al., 2015), reinforcing the importance of addressing these hazards early in site selection. Similarly, repeated fire activity on dry peatlands, as captured by MODIS and VIIRS satellite sensors, signals strong recurrent risk (Kiely et al., 2021). The GHI gradient demonstrates medium-level stability, justifying its role as an enhancer factor (ESMAP, 2019b).

In the context of agrivoltaic development, prioritizing evidence where microclimatic modifications provided by PV canopies such as reducing heat stress and lower evapotranspiration, which highlight meaningful agronomic benefits when the site is buildable and water access is manageable (Amaducci et al., 2018; Barron-Gafford et al., 2019). Ultimately, it reflects a balanced strategy that integrates technical practicality, ecological safety, and sustainable resource utilization in degraded peatland case.

Energy Yield, Land Use, and Emissions Avoidance

The effects of using agrivoltaics on technology and the environment could be obtained by turning information about where it can be used into how much energy it could produce and how much greenhouse gas it could keep from being released. 66,665.25 hectares of damaged peatland that are "Highly Suitable," which is about 666.65 square kilometers, was found. Using a careful estimate of 20 MW per square kilometer for how much power agrivoltaics can produce, we can approximate how much power could be installed in theory. This amount is often used in studies about big agrivoltaic systems that have tall structures and lots of space between rows. This setup lets farming happen under the panels (Amaducci et al., 2018; Weselek et al., 2021). These setups usually cover 25–35% of the ground and have rows spaced 6–10 meters apart. This balances using the land for farming, letting machines move around, and doing maintenance, while still having enough solar panels to make it worth the cost. This power amount is less than the roughly 35–50 MW per square kilometer that regular ground-based solar plants produce. But this difference shows that agrivoltaics is about using

land for two purposes, focusing on keeping the land productive in the long run, helping the environment, and helping local people.

Using this amount gives us a possible installed power of about 13.33 GW (666.65 × 20 MW). This is the possible power after considering things like natural reserves, protected areas, and limits because of infrastructure. To get exactly this much power, it's necessary to slowly build in areas that are close together and very suitable. This would need careful engineering plans, including service roads, checking how stable the peat soil is, and studying how to connect to the power grid to best increase power production. If this much power was used, approximately about 1.814 TWh (1,814 GWh) of electricity could be produced each year. This is based on making about 1,360 MWh per MWp per year, which matches how much sunlight there is in Southeast Asia and what has been seen in real-world tropical agrivoltaic projects (Barron-Gafford et al., 2019; Widmer et al., 2024).

The advantages for the climate from putting these plans into action are also very important. If we assume that the energy being replaced mainly comes from fossil fuels, which is likely true for Indonesia where coal is still the main power source, every megawatt of solar power could stop about 1,000 tons of CO_2 from entering the atmosphere each year (IEA, 2020; WattTime, 2020). This means that the areas best suited for solar power alone could prevent about 1.33 million tons of CO_2 from being released each year, which is the same as taking about 289,000 cars off the streets every year ($1.33\times10^6 \div 4.6$ tCO_2/vehicle/year), (U.S. EPA, 2025a, 2025b). These numbers are similar to what global studies say about how much solar panels can reduce emissions over their lifetime, with estimates of 800–1,100 tons of CO_2 prevented per megawatt each year, depending on how much carbon the replaced energy source creates (Merrouni et al., 2018; Columbia Sabin Center, 2022).

Also, if we consider the possible benefits of combining this with carbon storage from plants grown in peatlands like Metroxylon sagu or Melaleuca cajuputi, the total positive impact on the climate could be much greater, showing how well these combined solar and peatland systems could help. Looking at how the land is used, putting solar panels on farmland is a good use of space, even with careful spacing. Estimates of 8–12 hectares needed for each megawatt mean that a 1,333 megawatt system would need about 13,330 hectares (around 133.3 square kilometers), which is less than 20% of the total area considered "Highly Suitable". This suggests that not having enough land is not a problem, and much more solar power could be added without taking over important natural or farming areas. This idea matches what global studies have found, showing that large solar farms use a relatively small amount of land compared to energy from plants or water, and that using land for both farming and solar power can further reduce problems with land use by keeping farms productive (Dinesh & Pearce, 2016; Hernandez et al., 2015).

Co-benefits through Paludiculture Integration

One of the biggest changes that agrivoltaics can bring to peatlands is their ability to use land for many purposes, an idea that is increasingly called paludivoltaics. This idea is more than just putting farming and solar power together; it sees the solar setup as a way to fix the environment, lessen climate change, and help rural areas all at once. By raising solar panels and spacing rows far apart, agrivoltaic systems can keep the water levels and space needed to grow wetland crops like sago (Metroxylon sagu), gelam (Melaleuca cajuputi), and purun (Lepironia articulata), and also allow for fish farming and managed bodies of water. These plants, used for a long time in traditional wetland farming, are good at living in very wet places and can provide different kinds of natural products, such as sago flour, important oils, fibers for crafts, and fish as a protein source (Wichtmann et al., 2016; Joosten et al., 2016). This variety of income streams makes local communities more able to bounce back from problems, especially in faraway peatland areas where there are not many ways to make a living.

The small changes in climate caused by agrivoltaic setups make these benefits even greater. By making some shade and changing how energy moves on the surface, solar panels lower how much water evaporates and keep soil temperatures more steady, which helps keep water in the ground and reduces heat stress on

plants (Barron-Gafford et al., 2019; Widmer et al., 2024). This control of the local climate is very helpful in damaged peat areas, where plants struggle to grow back and crops do not produce well because of high surface temperatures and changing water levels. For crops that can handle shade, studies have shown that they grow just as well or even better under agrivoltaic conditions, which shows that using land for both energy and food does not have to be a competition, but can actually help both (Dinesh & Pearce, 2016; Amaducci et al., 2018).

Newer design ideas improve this connection even more by clearly making the light good for both plants and solar panels. Measurements like the Light Productivity Factor (LPF), created by Riaz et al. (2021), show how well sunlight is divided between what plants need for photosynthesis and how much electricity solar panels make. By changing things like the angle, space between rows, panel height, and direction, using LPF helps agrivoltaic systems go past simple design choices and instead get the best joint production. This way of thinking not only makes the whole system work better but also helps it last longer by matching technology with nature and farming needs. Adding wetland farming into agrivoltaic plans also offers big environmental advantages.

Plants like sago and purun that grow in wetlands are important for making peat and keeping the ground steady, which helps store carbon and lowers the chance of sinking land (Wichtmann et al., 2016; Mezbahuddin et al., 2023). Also, by keeping the ground wet, wetland farming lowers the risk of peat breaking down and big fires, which could really cause greenhouse gases to be released in Southeast Asian peatlands (Kiely et al., 2019). So, wetland-based solar systems not only work as renewable energy projects but also help fix ecosystems and fight climate change on a large scale. Looking at the bigger picture of society and the economy, the wetland solar idea fits with changing global sustainability ideas that focus on sharing land instead of saving it, and making landscapes that do many things at once, like provide food, energy, and environmental benefits all together (FAO, 2021). By turning damaged peatlands from wasted, fire-risky problems into useful and environmentally helpful assets, wetland solar systems show a big change in how renewable energy systems can be used — not as something that fights with farming or saving nature, but as something that helps both. This combined way puts agrivoltaics into the larger change toward a bioeconomy, making it more important for policy and more likely to be used in national plans for fixing land, energy, and the climate. A key aspect of combining farming and solar panels on peatlands is how they can be used for many purposes by combining renewable energy with farming methods that suit wetlands. Having lots of space between rows and raising solar panels up high makes it easier to grow sago, gelam, purun, and water-based plants, which can lead to earning money in different ways like from sago flour, oils, and fish. These added advantages help communities become stronger and help bring back ecosystems. It seems that using farming and solar panels together can make growing conditions better by lowering water loss and reducing heat problems, which helps keep the amount of crops steady for plants that can handle shade.

Hydrological and Geomorphic Constraints

To properly set up farming and solar panels together in swampy areas, it is important to think about water and land features to stop damage. Keeping the water level in the ground between –10 cm and –40 cm when it is not raining is key to stopping the swampy ground from breaking down, sinking, and catching fire more easily (Joosten et al., 2016). Making sure the ground sinks less than 2–3 cm each year is a smart rule to follow for keeping things steady for a long time (Mezbahuddin et al., 2023). These limits act like nature's filters: places that fit the rules for technology and resources but cannot keep the water conditions right should not be built on. Adding these details to how we decide where things can go makes choosing locations stronger and more lasting. Also, the consistent locations of swamp fires — shown by looking at fire data using special maps — are strong signs of repeated danger, while flood risks in low-lying areas have expected patterns in time and space that must be handled early when making choices

(Giglio et al., 2016; Alfieri et al., 2015; Kiely et al., 2019).

Novelty, Policy Implications, and Validation Pathways

GIS–AHP PV siting at provincial to national scales in arid and semi-arid settings commonly prioritizes GHI as the dominant weighted criterion (Al Garni & Awasthi, 2017; Giamalaki & Tsoutsos, 2019; Çolak et al., 2020), with local adjustments such as atmospheric dust weighting in Isfahan (Zoghi et al., 2017) or grid-proximity emphasis in coastal urban contexts where interconnection costs are high (Doorga et al., 2019). In island and developing-country contexts, fuzzy-MCDA variants and AHP combined with WLC are also prevalent (Yousefi et al., 2018; Merrouni et al., 2018), yet they remain largely resource-first. This study departs from that mainstream in two principal ways:

1. A degraded-first domain on tropical peat is enforced as the analysis mask from the outset, so the suitability map does not encourage expansion into intact peat but locks priorities to zones that are more negotiable ecologically and regulatorily.
2. A risk-first weighting order is adopted, with fire, flood, and geotechnical considerations upstream and GHI as an enhancer downstream, producing kilometre-scale contiguous clusters of Highly Suitable areas rather than isolated peaks in the brightest pixels.

The policy implications are direct. The mapping serves as a transparent, replicable first-pass screen to prioritize ground-truthing and pilot preparation at the tens-of-hectares scale, aligned with peat restoration efforts and rewetting or fire-break corridors that can be integrated into agrivoltaic design. The recommended validation agenda includes seasonal groundwater table profiling for depth and variability, site-specific geotechnical testing for bearing capacity and subsidence, access audits covering road and bridge classes, and verification of historical fire footprints within operational buffers. Because AHP weights are reported with CR and all criterion transformations are documented, data updates for hazard, access, or GHI can be propagated through the WLC without altering the geoprocessing design, making the framework auditable and adaptable. This study acknowledges that there are some things it does not do well. The amount of pollution prevented (~1,000 tCO_2e for each MWp) is based on broad guesses and could change based on the makeup of the power system and small changes in pollution amounts. Information from real-world tests of farming-friendly solar setups on ruined peatlands is still limited, and differences in how well crops can handle things, water flow, and soil conditions at different places may change the results. Also, the cost to connect to the power grid and limits on how much power the grid can handle were not considered in the current setup. Even with these shortcomings, the research gives a repeatable, clear, and flexible method that links where things can be placed on a map with how much power they can produce, how much carbon they can cut, and how they can help society and the environment together, which is a good starting point for more research and government planning.

CONCLUSION

Based on the results and discussion, the conclusions of this study can be summarized as follows:

1. Suitability over 124,007.76 ha of degraded peatland in South Sumatra indicates that 78.65% (97,533.09 ha) falls within the “Suitable” to “Highly Suitable” range, with the “Highly Suitable” class dominating at 53.76% (66,665.25 ha). These results demonstrate substantial available space for agrivoltaic development on degraded land without exerting pressure on intact peat ecosystems.
2. The GIS–AHP–MCDA application produced measured and internally consistent criterion weights (CR=0.00244), prioritizing fire hazard (0.1965), peat depth (0.1781), and flood susceptibility (0.1599) before the energy resource factor GHI (0.1099). The validity of these weights ensures transparent and replicable multicriteria integration, yielding a reliable suitability index for first-pass site screening.

3. Using a conservative agrivoltaic power density of 20 MW per km², the post-constraint technical potential is approximately 13.33 GW. This figure reflects space-based potential that has passed risk screening for fire, flooding or water table, geotechnics, topography, and access, indicating that degraded peatlands can meaningfully contribute to the energy mix, with ultimate realization contingent on prioritizing site clusters, structural and crop corridor design, and grid integration.

ACKNOWLEDGEMENTS

The author gratefully acknowledges the data and services provided by BIG, World Bank/ESMAP, Solargis, NASA FIRMS, BNPB–InaRISK, OpenStreetMap contributors, BRGM, KLHK, BBSDLP, UNEP-WCMC, and IUCN (2023), as well as the developers of the GIS software used in this study.

REFERENCES

Al Garni, H. Z., & Awasthi, A. (2017). Solar PV power plant site selection using a GIS–AHP approach with application in Saudi Arabia. *Applied Energy, 206*, 1225–1240. https://doi.org/10.1016/j.apenergy.2017.10.024

Alfieri, L., Burek, P., Feyen, L., & Forzieri, G. (2015). Global warming increases the frequency of river floods in Europe. *Hydrology and Earth System Sciences, 19*, 2247–2260. https://doi.org/10.5194/hess-19-2247-2015

Amaducci, S., Yin, X., & Colauzzi, M. (2018). Agrivoltaic systems to optimise land use for electric energy production. *Applied Energy, 220,* 545–561. https://doi.org/10.1016/j.apenergy.2018.03.081

Badan Nasional Penanggulangan Bencana (BNPB). (n.d.). *InaRISK: Indonesia's Disaster Risk Assessment Portal [Data portal]*. Retrieved October 7, 2025, from https://inarisk.bnpb.go.id/

Barron-Gafford, G. A., Minor, R. L., Allen, N. A., Cronin, A. D., Brooks, A. E., & Pavao-Zuckerman, M. A. (2019). Agrivoltaics provide mutual benefits across the food–energy–water nexus in drylands. *Nature Sustainability, 2,* 848–855. https://doi.org/10.1038/s41893-019-0364-5

Baykal, T. M., et al. (2025). Performance assessment of GIS-based spatial clustering methods in forest fire data. *Natural Hazards*. https://doi.org/10.1007/s11069-025-07135-0

Çolak, H. E., Memişoğlu, T., & Gerçek, Y. (2020). Optimal site selection for solar photovoltaic (PV) power plants using GIS and AHP: A case study of Malatya Province, Turkey. *Renewable Energy, 149,* 565–576. https://doi.org/10.1016/j.renene.2019.12.078

Columbia Sabin Center. (2022). Solar panels reduce CO_2 emissions more per acre than trees. Retrieved from https://blogs.law.columbia.edu/climatechange/2022/10/25

Deng, H., Li, D., Cai, S., Zhao, F.. (2025). Spatio-temporal dynamics of forest fire occurrence in Yunnan, China from 2001 to 2021 based on MODIS. *npj Natural Hazards, 2,* Article 52. https://doi.org/10.1038/s44304-025-00102-6

Dinesh, H., & Pearce, J. M. (2016). The potential of agrivoltaic systems. *Renewable and Sustainable Energy Reviews, 54,* 299–308. https://doi.org/10.1016/j.rser.2015.10.024

Doljak, D., & Stanojević, G. (2017). Evaluation of natural conditions for site selection of ground-mounted photovoltaic power plants in Serbia. *Energy, 127,* 291–300. https://doi.org/10.1016/j.energy.2017.03.140

Doorga, J. R. S., Rughooputh, S. D. V., & Boojhawon, R. (2019). Multi-criteria GIS-based modelling technique for identifying potential solar farm sites: A case study in Mauritius. *Renewable Energy, 133,* 1201–1219. https://doi.org/10.1016/j.renene.2018.08.105

ESMAP. (2019a). *Global Solar Atlas 2.0: Technical report*. Washington, DC: World Bank.

ESMAP. (2019b). *Validation report for global solar radiation model* (Global Solar Atlas 2.0). Washington, DC: World Bank. https://documents.worldbank.org/curated/en/507341592893487792/pdf/Global-Solar-Atlas-2-0-Validation-Report.pdf

Food and Agriculture Organization of the United Nations (FAO). (2021). *The state of the world's land and water resources for food and agriculture: Systems at breaking point (SOLAW 2021) – Synthesis report.* Rome: FAO.

Finlayson, R. (2021). Managing peatlands in Indonesia's South Sumatra for multiple benefits. *CIFOR-ICRAF Forests News.*

Giamalaki, M., & Tsoutsos, T. (2019). Sustainable siting of solar power installations in the Mediterranean using GIS/AHP. *Renewable Energy, 141*, 64–75. https://doi.org/10.1016/j.renene.2019.03.100

Giglio, L., Schroeder, W., & Justice, C. O. (2016). The collection 6 MODIS active fire detection algorithm and fire products. *Remote Sensing of Environment, 178,* 31–41. https://doi.org/10.1016/j.rse.2016.02.054

Goepel, K. D. (2018). Implementation of an online software tool for the Analytic Hierarchy Process (AHP-OS). *International Journal of the Analytic Hierarchy Process, 10*(3), 469–487. https://doi.org/10.13033/ijahp.v10i3.590

Hernandez, R. R., Easter, S. B., Murphy-Mariscal, M. L., Maestre, F. T., Tavassoli, M., Allen, E. B., Barrows, C. W., Belnap, J., Ochoa-Hueso, R., Ravi, S., & Allen, M. F. (2015). Environmental impacts of utility-scale solar energy. *Renewable and Sustainable Energy Reviews, 29,* 766–779. https://doi.org/10.1016/j.rser.2013.08.041

Hooijer, A., Page, S., Jauhiainen, J., Lee, W. A., Lu, X. X., Idris, A., & Anshari, G. (2012). Subsidence and carbon loss in drained tropical peatlands. *Biogeosciences, 9*(3), 1053–1071. https://doi.org/10.5194/bg-9-1053-2012

International Energy Agency (IEA). (2023). *World Energy Outlook 2023.* Paris: IEA.

International Energy Agency (IEA). (2020). Annual direct CO_2 emissions avoided per 1 GW of installed capacity by technology and displaced fuel. International Energy Agency.

Intergovernmental Panel on Climate Change (IPCC). (2022). *AR6 WGIII: Mitigation of Climate Change.* Cambridge: Cambridge University Press.

Intergovernmental Panel on Climate Change (IPCC). (2023). *AR6 Synthesis Report.* Geneva: IPCC.

Irfan, M., Khakim, M. Y. N., Mardiansyah, W., Kurniawati, N., Awaluddin, Sulaiman, A., Iskandar, I., Suwignyo, R. A., Yang, H., & Choi, E. (2025). Peatland hydro-climatological parameters variability in response to 2019–2022 climate anomalies in the OKI Regency. *Atmosphere, 16*(1), 81. https://doi.org/10.3390/atmos16010081

Joosten, H., Tanneberger, F., & Moen, A. (Eds.). (2016). *Mires and peatlands of Europe: Status, distribution and conservation.* Stuttgart: Schweizerbart Science Publishers.

Kiely, L., Spracklen, D. V., Arnold, S. R., Papargyropoulou, E., Conibear, L., Wiedinmyer, C., Knote, C., Adrianto, H. A. (2021). Assessing costs of Indonesian fires and the benefits of restoring peatland. Nature Communications, 12, 7044. https://doi.org/10.1038/s41467-021-27353-x

Kiely, L., Spracklen, D. V., Wiedinmyer, C., Conibear, L., Reddington, C. L., Archer-Nicholls, S., Lowe, D., Arnold, S. R., Knote, C., Khan, M. F., Latif, M. T., Kuwata, M., Budisulistiorini, S. H., & Syaufina, L. (2019). New estimate of particulate emissions from Indonesian peat fires in 2015. *Atmospheric Chemistry and Physics, 19*, 11105–11121. https://doi.org/10.5194/acp-19-11105-2019

Kırcalı, Ş., & Selim, S. (2021). Site suitability analysis for solar farms using the geographic information system and multi-criteria decision analysis: The case of Antalya, Turkey. *Clean Technologies and Environmental Policy, 23*(4), 1233–1250. https://doi.org/10.1007/s10098-020-02018-3

Kurniawan, I., Ichwani, R., Aryansyah, Fionasari, R., & Huda, A. (2024). The implementation of export–import (E–I) subsidies regulation on rooftop photovoltaic plant system in Indonesia based on techno-economic point of view: A study case in Ogan Komering Ulu Region, South Sumatera, Indonesia. *International Journal of Sustainable Development and Planning, 19*(4), 1371–1378. https://doi.org/10.18280/ijsdp.190414

Kocabaldır, C., & Yücel, M. A. (2023). GIS-based multicriteria decision analysis for spatial planning of solar photovoltaic power plants in Çanakkale province, Turkey. *Renewable Energy, 212,* 455–467. https://doi.org/10.1016/j.renene.2023.05.075

Merrouni, A., Ghazanfari, A., & Amara, M. (2018). Large-scale PV sites selection by combining GIS and the Analytic Hierarchy Process: Case study of Eastern Morocco. Renewable Energy. https://doi.org/10.1016/j.renene.2017.10.044

Mezbahuddin, S., Nikonovas, T., Spessa, A., Grant, R. F., Imron, M. A., Doerr, S. H., Clay, G. D. (2023). Accuracy of tropical peat and non-peat fire forecasts enhanced by simulating hydrology. *Scientific Reports, 13,* Article 619. https://doi.org/10.1038/s41598-022-27075-0

NASA. (n.d.). *Fire Information for Resource Management System (FIRMS) [Data set]*. NASA Earthdata/LANCE. Retrieved October 7, 2025.

NASA. (n.d.). *LANCE | FIRMS*. Retrieved October 7, 2025, from https://firms.modaps.eosdis.nasa.gov/

Noorollahi, E., Ghodsipour, S. H., & Yousefi, A. (2016). Land suitability analysis for solar farms exploitation using GIS and fuzzy AHP. *Energies, 9*(8), 643. https://doi.org/10.3390/en9080643

OpenStreetMap contributors. (2025). *OpenStreetMap [Data set]*. OpenStreetMap Foundation. Retrieved October 7, 2025, from https://www.openstreetmap.org

Riaz, H., Imran, H., Alam, H., Alam, M. A., & Butt, N. Z. (2021). Crop-specific optimization of bifacial PV arrays for agrivoltaic production. arXiv preprint arXiv:2104.00560. https://doi.org/10.48550/arXiv.2104.00560

Saaty, T. L. (1980). *The Analytic Hierarchy Process.* New York: McGraw-Hill.

Saaty, T. L. (2008). Decision making with the analytic hierarchy process. *International Journal of Services Sciences, 1(1),* 83–98. https://doi.org/10.1504/IJSSCI.2008.017590

UNEP-WCMC, & IUCN. (2023). *Protected Planet: The World Database on Protected Areas (WDPA).* Cambridge: UNEP-WCMC & IUCN.

U.S. Environmental Protection Agency. (2025a). *Greenhouse gas emissions from a typical passenger vehicle.* https://www.epa.gov/greenvehicles/greenhouse-gas-emissions-typical-passenger-vehicle

U.S. Environmental Protection Agency. (2025b). *Greenhouse gas equivalencies calculator.*

Vernimmen, R., Hooijer, A., Akmalia, R., Giesen, W., Dommain, R., Rompas, A., & Silvius, M. (2020). Mapping deep peat carbon stock from a LiDAR-based DTM and field measurements, with application to eastern Sumatra. *Carbon Balance and Management, 15*(1), 19. https://doi.org/10.1186/s13021-020-00139-2

WattTime. (2020). Lifecycle and avoided emissions of solar technologies. Retrieved from https://watttime.org

Weselek, A., Ehmann, A., Ziegler, M., Lewandowski, I., & Högy, P. (2021). Agrivoltaic system impacts on microclimate and yield of different crops within an organic crop rotation in a temperate climate. *Agronomy for Sustainable Development, 41,* 59. https://doi.org/10.1007/s13593-021-00714-y

Wichtmann, W., Schröder, C., & Joosten, H. (Eds.). (2016). *Paludiculture – Productive use of wet peatlands: Climate protection – biodiversity – regional economic benefits.* Stuttgart: Schweizerbart Science Publishers.

Widmer, J., Christ, B., Grenz, J., & Norgrove, L. (2024). Agrivoltaics, a promising new tool for electricity and food production: A systematic review. *Renewable and Sustainable Energy Reviews, 192*, Article 114277. https://doi.org/10.1016/j.rser.2023.114277

World Bank Group; Solargis. (2023). *World – Global Horizontal Irradiation (GHI) GIS data (Global Solar Atlas) [Data set]*. EnergyData.info. Retrieved October 7.

Yousefi, H., Hafeznia, H., & Yousefi-Sahzabi, A. (2018). Spatial Site Selection for Solar Power Plants 2025Using a GIS-Based Boolean-Fuzzy Logic Model: A Case Study of Markazi Province, Iran. *Energies, 11*(7), 1648. https://doi.org/10.3390/en11071648

Zoghi, M., Ehsani, A. H., Sadat, M., Amiri, M. J., & Karimi, S. (2017). Optimization of solar site selection by fuzzy logic model and weighted linear combination method in arid and semi-arid region: A case study in Isfahan, Iran. *Renewable and Sustainable Energy Reviews, 68,* 986–996. https://doi.org/10.1016/j.rser.2015.07.014